J|A|C|S
ARTICLES
Published on Web 01/31/2002

Exchange Interactions in the Three Phases of Vanadyl Pyrophosphate $(VO)_2P_2O_7$

Sébastien Petit,[†] Serguei A. Borshch,[†] and Vincent Robert*[,†,‡]

Contribution from the Institut de Recherches sur la Catalyse, UPR 5401, 2, Avenue Albert Einstein, 69626 Villeurbanne Cedex, France, Ecole normale supérieure de Lyon, Laboratoire de Chimie Théorique, 46, allée d'Italie, 69364 Lyon Cedex 07, France, and Université Claude Bernard de Lyon I, 43, boulevard du 11 novembre 1918, 69622 Villeurbanne Cedex, France

Received July 25, 2001. Revised Manuscript Received October 29, 2001

Abstract: The magnetic exchange constants of vanadyl pyrophosphate $(VO)_2P_2O_7$ have been calculated on the basis of a combined DFT/broken symmetry approach. The three reported phases, ambient-pressure orthorhombic, ambient-pressure monoclinic, and high-pressure orthorhombic, have been explicitly considered. Calculations have been performed on four types of model clusters extracted from the crystal lattices. The singularity of each phase is clearly reflected through the number and values of exchange parameters. Our results show that the exchange interactions can be described in first approximation within the alternating antiferromagnetic chain model. The largest exchange coupling along the chain occurs through O−P−O bridges. The interchain interactions are much weaker and are of ferromagnetic nature.

1. Introduction

Vanadyl(IV) pyrophosphate $(VO)_2P_2O_7$ is one of the most studied catalytic solids.[1−3] It is the principal component of an active catalyst in the industrial synthesis of maleic anhydride from *n*-butane. This particular reaction involves a 14-electron oxidation and the abstraction of eight protons. Even though several phase transformations are likely to occur along the reaction, the nature of the active site originated from $(VO)_2P_2O_7$ has not been clarified so far. As a consequence of such a complex system, a large range of experimental techniques[1−12] and theoretical approaches[13−16] has been called for to elucidate the active phase structure and the actual reaction path.

In the meantime, vanadyl pyrophosphate has been much debated within the context of low dimensional magnetic systems.[16−23] Each vanadium site in the formal oxidation state V^{4+} has a d^1 electronic configuration and a local spin of $^1/_2$. These paramagnetic centers can be linked in the crystal structure of $(VO)_2P_2O_7$ through different exchange pathways giving rise to specific magnetic properties. The magnetic interaction scheme has been studied in the literature for more than 10 years since the lattice structure was first determined by Gorbunova et al. (Figure 1).[24a]

For several years, this ambient-pressure orthorhombic phase (APO) was considered as the first example of an inorganic two-leg spin ladder system (Figure 1a). This one-dimensional magnetic system is formed by the stacking of di-μ-oxo vanadium dimers D_O along the **a** direction of the crystal. However, the crystal structure along the **b** direction is suggestive of quite another magnetic spin system, an alternating dimer chain (Figure 1b). The latter results from the alternation of D_O and O−P−O-bridged dimers D_{OPO}. These two Heisenberg-type models are based on different hierarchies for the exchange interactions. If

* To whom correspondence should be addressed. E-mail: vrobert@ens-lyon.fr. Fax: (33) 4 72 44 53 99.
† Institut de Recherches sur la Catalyse.
‡ Université Claude Bernard de Lyon I.

(1) Forum on vanadyl pyrophosphates catalysts: Centi, G. , Ed. *Catal. Today* (special issue) **1993**, *16*, 1−147.
(2) Trifiro, F.; Centi, G.; Ebner, J. R.; Franchetti, V. M. *Chem. Rev.* **1988**, *88*, 55.
(3) Bordes, E. *Catal. Today* **1987**, *1*, 499.
(4) Abdelouahab, F. B.; Olier, R.; Guilhaume, N.; Lefebvre, F.; Volta, J.-C. *J. Catal.* **1992**, *134*, 151.
(5) Vedrine, J.-C.; Millet, J.-M.; Volta, J.-C. *Faraday Discuss. Chem. Soc.* **1989**, *87*, 207.
(6) Sananes, M. T.; Tuel, A.; Volta, J.-C. *J. Catal.* **1994**, *145*, 251.
(7) Li, J.; Lashier, M. E.; Schrader, G. L.; Gerstein, B. B. *Appl. Catal.* **1991**, *73*, 83.
(8) Rodemerck, U.; Kubias, B.; Zanthoff, H.-W.; Baerns, M. *Appl. Catal., A* **1997**, *153*, 203.
(9) Zazhigalov, V. A.; Haber, J.; Stoch, J.; Bogutskaya, L. V.; Bacherikova, I. V. *Appl. Catal., A* **1996**, *135*, 155.
(10) Agaskar, P. A.; DeCaul, L.; Grasselli, R. K. *Catal. Lett.* **1994**, *23*, 339.
(11) Johnson, J. W.; Johnston, D. C.; Jacobson, A. J.; Brody, J. F. *J. Am. Chem. Soc.* **1984**, *106*, 8123.
(12) Johnston, D. C.; Johnson, J. W. *J. Chem. Soc., Chem. Commun.* **1985**, 1720.
(13) Schiott, B.; Jorgensen, K. A.; Hoffmann, R. *J. Phys. Chem.* **1991**, *95*, 2297.
(14) Robert, V.; Borshch, S. A.; Bigot, B. *Chem. Phys.* **1996**, *210*, 401.
(15) Robert, V.; Borshch, S. A.; Bigot, B. *J. Mol. Catal. A: Chem.* **1997**, *119*, 327.
(16) Witko, M.; Tokarz, R.; Haber, J.; Hermann, K. *J. Mol. Catal. A: Chem.* **2001**, *166*, 59.
(17) Johnston, D. C.; Johnson, J. W.; Goshorn, D. P.; Jacobson, A. J. *Phys. Rev. B* **1987**, *35*, 219.
(18) Barnes, T.; Dagotto, E.; Riera, J.; Swanson, E. S. *Phys. Rev. B* **1993**, *47*, 3196.
(19) Barnes, T.; Riera, J. *Phys. Rev. B* **1994**, *50*, 6817.
(20) Garrett, A. W.; Nagler, S. E.; Barnes, T.; Sales, B. C. *Phys. Rev. B* **1997**, *55*, 3631.
(21) Garrett, A. W.; Nagler, S. E.; Tennant, D. A.; Sales, B. C.; Barnes, T. *Phys. Rev. Lett.* **1997**, *79*, 745.
(22) Kikuchi, J.; Motoya, K.; Yamauchi, T.; Ueda, Y. *Phys. Rev. B* **1999**, *60*, 6731.
(23) Yamauchi, T.; Narumi, Y.; Ueda, Y.; Tatani, K.; Kobayashi, T. C.; Kindo, K.; Motoya, K. *Phys. Rev. Lett.* **1999**, *83*, 3729.
(24) (a) Gorbunova, Y. E.; Linde, S. A. *Sov. Phys. Dokl.* **1979**, *24*, 138. (b) Hiroi, Z.; Azuma, M.; Fujishiro, Y.; Saito, T.; Takano, M.; Izumi, F.; Kamiyama, T.; Ikeda, D. *J. Solid State Chem.* **1999**, *146*, 369.

10.1021/ja011812d CCC: $22.00

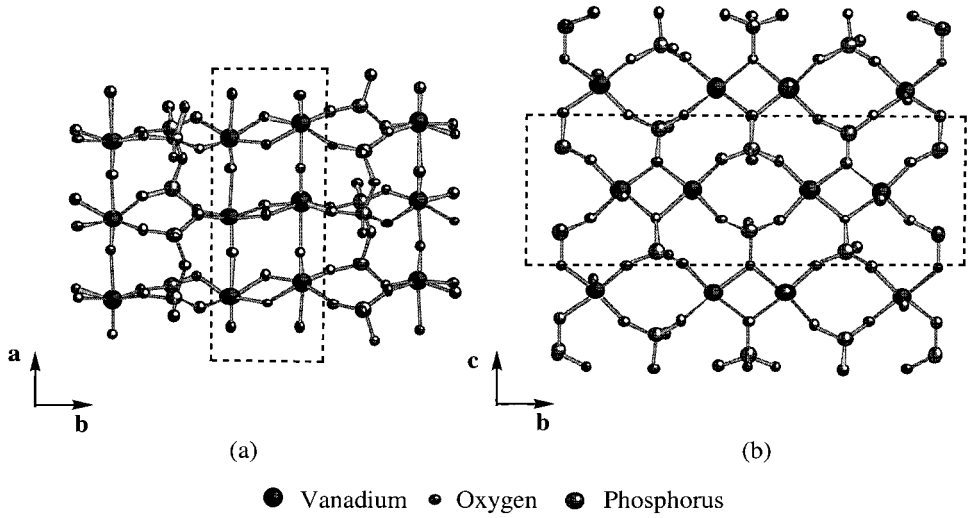

Figure 1. (a) $(VO)_2P_2O_7$ spin ladder structure along the **a** direction in the APO phase. (b) Alternating dimer chain along the **b** direction. The rectangles show the constitutive dimeric units.

J'_O stands for the exchange constant through vanadyl oxygen along the **a** direction, the spin ladder model is consistent with $|J'_O|$, $|J_O| \gg |J_{OPO}|$, whereas the dimer chain model assumes $|J_{OPO}|$, $|J_O| \gg |J'_O|$.

Surprisingly, the magnetic susceptibility versus temperature data were accurately reproduced by both models. Originally, Johnston et al.[17] fitted their results by an antiferromagnetic alternating spin chain, and a few years later Barnes et al.[18] suggested that the two approaches be confronted. The concept of the $(VO)_2P_2O_7$ APO phase being an alternating chain compound started to be widely accepted when the measurement of magnetic excitations by inelastic neutron scattering (INS) revealed the strongest antiferromagnetic interactions along the *b* axis.[21] The authors pointed out that the exchange constants J_O and J_{OPO} were of the same order of magnitude, whereas J'_O was negligibly small. Another important experimental finding is the coexistence of two singlet−triplet excitation gaps (36 and 67 K) which were attributed to the presence of two chains exhibiting slightly different structural parameters.[22,23] Depending on the preparation method, vanadyl pyrophosphate can crystallize in an ambient-pressure monoclinic phase (APM), the structure of which was reported by Nguyen et al.[25] Two inequivalent dimer chains are present in both structures APO and APM. On annealing under high-pressure (3 GPa), the APO phase transforms into a simplified structure, the high-pressure orthorhombic phase (HPO).[26] As a main consequence of this transformation, the magnetic susceptibility and heat capacity measurements indicate only one spin gap (27 K). The exchange parameters obtained for the different $(VO)_2P_2O_7$ phases are given in Table 1. One should note that these values depend on the experimental methods as well as on the imposed theoretical models (one or two chains, with/without interchain interactions).

The interests of catalytic and magnetic research communities overlap when NMR data of paramagnetic compounds are to be interpreted. Magic angle spinning and spin−echo mapping techniques for the ^{31}P nucleus have been extensively used to characterize the different vanadium phosphorus oxide phases which may take part in the catalytic reaction.[6,7,27] The vanadium oxidation state is known to be +4 or +5 in the industrial catalyst. Resonance is reached around 0 ppm for vanadium V^{+5} species, whereas paramagnetic compounds V^{4+} exhibit large chemical shifts, varying in the range 2000−4500 ppm with a strong temperature dependency. Such high values certainly result from the contact term contribution into the hyperfine structure. A generally accepted interpretation lies in the presence of unpaired d electrons that polarize the inner s-shell giving rise to nonzero electronic density at the resonant site.

Traditional quantum approaches of chemical shifts which have been widely presented over the last years are not suitable for paramagnetic species.[28−30] An alternative approach to spin-coupled systems may lie in a combined method. The interacting spins system should be described on the basis of a Heisenberg Hamiltonian. As for the local nucleus−electronic spin density interaction, parameters can be extracted from experimental

Table 1. Experimental Values of *J* Parameters in Different Phases of VPO

phase	J_{OPO} (K)	J_O (K)	$J_{interchain}$ (K)	experimental method	reference
APO	130.9	102.4		magnetic susceptibility	24b
	136 (A) 124 (B)	92 (A) 103 (B)		NMR	22
	142.9 (A) 119.5 (B)	118.1 (A) 100.9 (B)	−3	INS	21
	132 (A) 111 (B)	112 (A) 110 (B)	10.9−17.1[a] 12.5−19.5[a]	Raman	50
HPO	131.6	114.6		magnetic susceptibility	26

[a] Raman data do not provide information about the sign of interchain exchange.

(25) Nguyen, P. T.; Hoffman, R. D.; Sleight, A. W. *Mater. Res. Bull.* **1995**, *30*, 1055.
(26) Saito, T.; Terashima, T.; Azuma, M.; Takano, M.; Goto, T.; Ohta, H.; Utsumi, W.; Bordet, P.; Johnston, D. C. *J. Solid State Chem.* **2000**, *153*, 124.
(27) Sananes, M. T.; Tuel, A. *Solid State Nucl. Magn. Reson.* **1996**, *6*, 157.
(28) Chesnut, D. B. The Ab Initio Computation of Nuclear Magnetic Resonance Chemical Shielding. In *Reviews in Computational Chemistry*; Lipkowitz, K. B., Boyd, D. B., Eds; Weinheim/VCH: New York, 1996; Vol. 8, p 245.
(29) Rauhut, G.; Puyear, S.; Wolinski, K.; Pulay, P. J. *J. Phys. Chem.* **1996**, *100*, 6310.
(30) Malkin, V. G.; Malkina, O. L.; Salahub, D. R. *J. Am. Chem. Soc.* **1995**, *117*, 3294.

data.[31] Recently, we have reported the analysis of four temperature-dependent NMR signals in $(VO)_2P_2O_7$ based on two different models for the exchange interaction's scheme. Although we were able to estimate combinations of hyperfine constants, the spin ladder and the dimer chain models led to very similar results.[32] Thus, the knowledge of the exchange interaction's topology and a quantitative evaluation of the exchange constants would be desirable for the interpretation of $(VO)_2P_2O_7$ NMR data. Such information can be provided by quantum chemical calculations of exchange constants.

This area of research has benefited a lot from the current use of density functional theory (DFT) calculations. Indeed, modern ab initio approaches (post Hartree−Fock) may fail to tackle large systems at a reasonable computational cost. The parameters for exchange interaction have been fairly reproduced in numerous polynuclear transition metal complexes as well as in fragments of solids.[33−40] Using this strategy, the influence of particular structural parameters on exchange coupling has been quantitatively described. For a large majority of studied systems, the generalized gradient-corrected hybrid functional B3-LYP gave the best results.

Recently, we performed DFT calculations of exchange parameters for the ambient-pressure monoclinic phase (APM) of vanadyl pyrophosphate.[41] The details of the solid-state structure were explicitly taken into account when constructing the model molecular fragments. The nature of the bridge (μ-oxo or O−P−O) and the positions of phosphorus atoms directly control the exchange parameters. We showed that even though the dimer chains involve alternating μ-oxo and O−P−O bridges, they are more properly described by three or four exchange parameters rather than by two. However, full agreement with the experiment was not reached, probably as a consequence of a different exchange-correlation functional we used. Recently, a qualitative analysis of the spin exchange interactions in the three phases (APM, APO, and HPO) has been suggested.[42] Spin exchange parameters of dimers have been discussed in terms of one-electron orbital energies from extended Hückel calculations. However, the lack of ab initio estimations of exchange values for these particular compounds still remains.

In the present article, we intend to bridge the gap between experimental magnetic data and their theoretical descriptions in vanadyl pyrophosphate phases. On the basis of DFT quantum calculations, exchange parameters for the three reported structures of different symmetries are presented. Intrachain as well as interchain coupling constants are estimated. Since all of the three phases exhibit similar molecular fragments organized differently in the crystal structure, their parallel analysis allows one to interpret and to clarify magnetostructural correlations in this important solid.

2. Theoretical Approach and Computational Details

The use of ab initio techniques to obtain satisfactory approximations of the spin eigenstates was a turning point in the evaluation of exchange coupling parameters. Numerous studies have shown the power of first principle calculations to accurately evaluate the magnetic interactions in binuclear complexes.[43−46] The degree of accuracy required for such evaluations disposes the extremely demanding multideterminant methods reported by several authors. However, Noodelman et al. proposed an alternative approach based on an unrestricted, or spin polarized, formalism (either Hartree−Fock (UHF) or density functional theory (DFT)).[33,34] A state of mixed spin symmetry is obtained by means of self-consistent procedure when the magnetic orbitals (singly occupied molecular orbitals, SOMOs) are allowed to interact. This method is referred to as "broken symmetry" calculations (BS). For a system consisting of two unpaired electrons in two nonorthogonal localized orbitals a and b (natural magnetic orbitals), the single determinant BS state can be written in a monodeterminant DFT approach as

$$|\mathrm{BS}\rangle = |a\bar{b}|/\sqrt{2} \tag{1}$$

and the magnetic coupling constant $J = E_S - E_T$ reads

$$J = \frac{2(E_{BS} - E_{T'})}{1 + S_{ab}^{\ 2}} \tag{2}$$

where S_{ab} stands for the integral overlap between a and b orbitals. If one assumes that spin contamination inherent to unrestricted formalism is small, T' is a good approximation for the pure triplet state T defining the magnetic coupling constant. However, much controversy remains as for the proper use of eq 2. It has been suggested[34,36] that magnetic orbitals calculated from DFT are much more delocalized, as opposed to those calculated from Hartree−Fock, and the overlap integral S_{ab} goes to unity resulting in

$$J = E_{BS} - E_{T'} \tag{3}$$

However, the so-called "weak bonding" regime introduced through perturbation theory by Noodelman,[33] where spin orbitals a and b are fully localized (strong correlation), leads to

$$J = 2(E_{BS} - E_{T'}) \tag{4}$$

It has been noticed[35,36] that the non spin-projected eq 3 led to the best estimation of the exchange parameter for some particular compounds in agreement with the experiments. We recently used this approach in our calculations of exchange constants in the APM phase. However, as noticed by Caballol et al.,[47] there is no physical justification to ignore the spin contamination in unrestricted calculations. In the present paper, we rather intend to consider the influence of the overlap amplitude.

All our calculations were performed using the Gaussian 98 package,[48] within the broken symmetry approach and rather extended basis sets.

(31) Mouesca, J.-M.; Noodleman, L.; Case, D. A.; Lamotte, B. *Inorg. Chem.* **1995**, *34*, 4347.
(32) Lawson Daku, M. L.; Borshch, S. A.; Robert, V.; Bigot, B. *Chem. Phys. Lett.* **2000**, *330*, 423.
(33) Noodleman, L. *J. Chem. Phys.* **1981**, *74*, 5737.
(34) Noodleman, L.; Norman, J. G. *J. Chem. Phys.* **1979**, *70*, 4903.
(35) Ruiz, E.; Alemany, P.; Alvarez, S.; Cano, J. *J. Am. Chem. Soc.* **1997**, *119*, 1297.
(36) Ruiz, E.; Cano, J.; Alvarez, S.; Alemany, P. *J. Comput. Chem.* **1999**, *20*, 1391.
(37) Adamo, C.; Barone, V.; Bencini, A.; Totti, F.; Ciofini, I. *Inorg. Chem.* **1999**, *38*, 1996.
(38) Ruiz, E.; Cano, J.; Alvarez, S.; Alemany, P.; Verdaguer, M. *Phys. Rev. B* **2000**, *61*, 54.
(39) Blanchet-Boiteux, C.; Mouesca, J.-M. *J. Am. Chem. Soc.* **2000**, *122*, 861.
(40) Blanchet-Boiteux, C.; Mouesca, J.-M. *J. Phys. Chem. A* **2000**, *104*, 2091.
(41) Lawson Daku, M. L.; Borshch, S. A.; Robert, V.; Bigot, B. *Phys. Rev. B* **2001**, *63*, 174439.
(42) Koo, H.-J.; Whangbo, M.-H. *Inorg. Chem.* **2000**, *39*, 3599.
(43) De Loth, P.; Cassoux, P.; Daudey, J. P.; Malrieu, J. P. *J. Am. Chem. Soc.* **1981**, *103*, 4007.
(44) Charlot, M. F.; Verdaguer, M.; Journaux, Y.; De Loth, P.; Daudey, J. P. *Inorg. Chem.* **1984**, *23*, 3802.
(45) Castell, O.; Caballol, R.; Garica, V. M.; Handrick, K. *Inorg. Chem.* **1996**, *35*, 1609.
(46) Castell, O.; Caballol, R. *Inorg. Chem.* **1999**, *38*, 668.
(47) Caballol, R.; Castell, O.; Illas, F.; Moreira, I de P. R.; Malrieu, J. P. *J. Phys. Chem. A* **1997**, *101*, 7860.
(48) Frisch, M. J.; Trucks, G. W.; Schlegel, H. B.; Scuseria, G. E.; Robb, M. A.; Cheeseman, J. R.; Zakrzewski, V. G.; Montgomery, J. A., Jr.; Stratmann, R. E.; Buran, J. C.; Dapprich, S.; Millam, J. M.; Daniels, A. D.; Kudin, K. N.; Strain, M. C.; Farkas, O.; Tomasi, J.; Barone, V.; Cossi, M.; Cammi, R.; Mennuci, B.; Pomelli, C.; Adamo, C.; Clifford, S.; Ochterski, J.; Peterson, G. A.; Ayala, P. Y.; Cui, Q.; Mokuma, K.; Malick, D. K.; Rabuk, A. D.; Raghavachari, K.; Foresman, J. B.; Cioslowski, J.; Ortiz, J. V.;

Double-ζ GTO basis sets, 6-31G, were used for H, O, and P atoms, extended with one polarization function for P. As far as the V atom is concerned, the effects of the core electrons up to 2p were accounted for with the Los Alamos pseudopotential. Double-ζ basis sets optimized for this particular effective core potential (ECP) were applied for the valence electrons. We used the standard generalized gradient-corrected hybrid functional B3-LYP, consisting of the exchange Becke three parameter functional and the Lee−Yang−Parr correlation functional. The comparison with our previous results for the vanadyl pyrophosphate APM phase[41] justifies this choice. As a starting point for the SCF procedure, the initial broken symmetry state was constructed by allowing the mixing of the highest α and β spin orbitals in the converged triplet state. The overlap elements were computed by means of a local software that has been developed for specific Gaussian basis sets used in the Gaussian 98 package.

3. Description of Molecular Models

The layered structure of the APO phase (Figure 1) is preserved in the APM and HPO phases.[25,26] The common motif of all layers is represented by a $VO(\mu_2 - O)_2$ VO unit, where the two vanadyl groups V═O are in an anti orthogonal configuration. These units are linked through O−P−O bridges giving rise to a quasi-monodimensional chain. In the APO and APM phases, the vanadyl bond orientations alternate up-down-down-up, whereas in the HPO phase the order is up-down-up-down. The crystal structures of the APO and APM phases contain two chain types in the *bc* plane with slightly different bond distances and valence angles.[24,25] However, the number of atoms in the APM phase elementary cell is twice that of the APO cell. Conversely, the HPO phase exhibits a single type of alternating chains.

Our analysis of exchange interactions in the three vanadyl pyrophosphate phases is based on electronic structure calculations of molecular fragments extracted from the crystal structures. In this approach, we assumed that the whole crystal potential can be neglected in the calculations if the coordination spheres are sufficiently extended. Magnetic measurements are obtained from solid samples where packing forces are likely to produce geometrical deviations from the isolated molecules. The high sensitivity of magnetic parameters to fine geometrical details of the local environment has been reported several times in the literature.[35,37,38] Therefore, the models we used were not optimized since these small variations may produce large changes in the calculated exchange constants.

As molecular fragments, we considered subunits consisting of two adjacent vanadium centers in all the possible exchange pathways. In this way we did not assume the presence of any dominating exchange coupling, but rather focused on the local structure characteristics of each phase. Four types of dimer have been identified in these solids. Therefore, the μ-oxo (D_O) (Figure 2) and O−P−O (D_{OPO}) (Figure 3) dimer types were considered to map out intrachain magnetic interactions along the **b** direction. One should stress that the D_{OPO} dimers display anti orthogonal and syn orthogonal configurations of vanadyl bonds in the high-pressure and low-pressure phases, respectively.

We were also concerned with interchain links in the *bc* plane through the O−P−O^C bridge (D^C_{OPO}) (Figure 4) and through the vanadyl bond along the **a** direction (D'_O) (Figure 5).

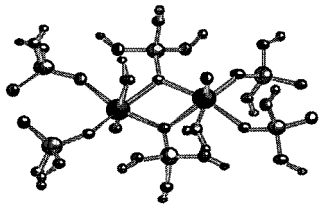

Figure 2. μ-Oxo dimer cluster model D_O.

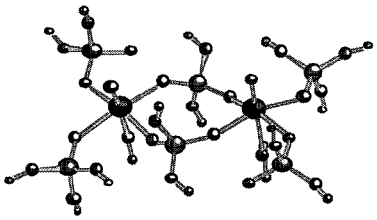

Figure 3. O−P−O dimer cluster model **II** D_{OPO}.

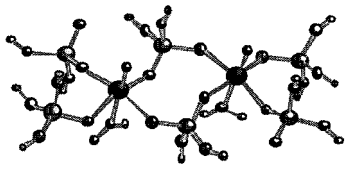

Figure 4. Dimer cluster model **II** D^C_{OPO} (in plane interchain interaction).

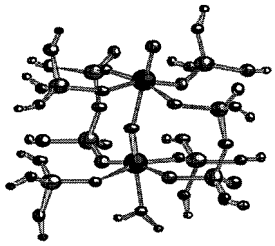

Figure 5. Dimer cluster model D'_O (through vanadyl interchain interaction).

The size of each dimeric unit was defined so as to take into consideration computational efficiency. However, the vanadium atoms' environments were extended up to third coordination spheres to include the influence of the long-range potentials on magnetic sites. Since the magnetic diversity is known to result from the participation of phosphate groups in the spin transfer,[49] special attention was paid to the description of these groups. In particular, the local environment of each phosphorus atom was taken from the crystallographic structures where two short (∼1.47 Å) and two long (∼1.55 Å) P−O distances are observed. By means of protons coordinated to oxygen atoms, the charge of our model complexes was set to zero. The exact positions of these hydrogen atoms are particularly important and may control the magnitude of exchange parameters. In this context, the phosphorus-bound oxygen atoms of D_O dimers were all saturated. As for D_{OPO} dimers, two different models were constructed. The first one (**I**) consists of two HPO_4^{2-} bridges and four H_3PO_4 units in trans positions to the former. Conversely, the second (**II**) results from the migration of two protons from H_3PO_4 units, leading to HPO_4^{2-} bridges. We should recall that we were concerned with depicting structurally equivalent subunits.

Stefanov, B. B.; Liu, G.; Liashenko, A.; Piskorz, P.; Komaromi, I.; Gomperts, R.; Martin, R. L.; Fox, D. J.; Keith, T.; Al-Laham, M. A.; Peng, C. Y.; Nanayakkara, A.; Gonzalez, C.; Challacombe, M.; Gill, P. M. W.; Johnson, B. G.; Chen, W.; Wong, M. W.; Andres, J. L.; Head-Gordon, M.; Replogle, E. S.; Pople, J. A. *Gaussian 98*, revision A.7; Gaussian, Inc.: Pittsburgh, PA, 1998.

(49) Roca, M.; Amoros, P.; Cano, J.; Marcos, D. M.; Alamo, J.; Beltran-Poter, A.; Beltran-Poter, D. *Inorg. Chem.* **1998**, *37*, 3167.

Table 2. Calculated Intrachain Exchange Parameters

phase		J (K)		J (K)[a]
HPO	D_O	105	D_{OPO}	144 (200)
APO	D_O^A	55	D_{OPO}^A	115 (172)
	D_O^B	110	D_{OPO}^B	145 (205)
APM	D_O^{A1}	70	D_{OPO}^{A1}	124 (176)
	D_O^{A2}	71	D_{OPO}^{A2}	124 (182)
	D_O^{B1}	79	D_{OPO}^{B1}	162 (223)
	D_O^{B2}	88	D_{OPO}^{B2}	170 (237)

[a] Exchange values are calculated with model **II** (model **I** in parentheses).

Table 3. Calculated Interchain Exchange Parameters

phase		J (K)		J (K)
HPO	D_{OPO}^C	−6	D_O'	−37
APO	D_{OPO}^{C1}	−12	D_O^1	−41
	D_{OPO}^{C2}	−9	D_O^2	−38
	D_{OPO}^{C3}	−13	D_O^3	−14
	D_{OPO}^{C4}	−13	D_O^4	−17
APM	D_{OPO}^{C1}	−14	D_O^1	−28
	D_{OPO}^{C2}	−14	D_O^2	−36
	D_{OPO}^{C3}	−13	D_O^3	−34
	D_{OPO}^{C4}	−15	D_O^4	−25
	D_{OPO}^{C5}	−13	D_O^5	−25
	D_{OPO}^{C6}	−12	D_O^6	−23
	D_{OPO}^{C7}	−14	D_O^7	−17
	D_{OPO}^{C8}	−12	D_O^8	−17

The number of similar dimers to be considered in each phase depends on the elementary cell size. For example, only one single D_O and D_{OPO} dimer can be defined for the HPO phase, whereas there are two and four dimers of each type for the APO and APM phases, respectively.

4. Results and Discussion

From our calculations, the largest exchange constants are attributed to the D_O and D_{OPO} dimers and correspond to antiferromagnetic interaction (positive *J* values with our convention). Therefore, the description of exchange interactions in $(VO)_2P_2O_7$ phases can be, in first approximation, directly deduced from the alternating antiferromagnetic chain model. The corresponding exchange parameters we calculated in the three different phases, APM, APO, and HPO, are given in Table 2.

The interchain exchange coupling represented by D_{OPO}^C and D_O' dimers is less important in magnitude (Table 3). One should stress that the corresponding values are all negative, a reflection of the ferromagnetic character of interchain coupling. The interchain ferromagnetic exchange interactions turn out to be the most efficient along the **a** direction (D_O' dimers). This result differs from those obtained on the basis of previous theoretical approaches.[41,49] We may argue that this discrepancy is due to the use of oversimplified structural models. First, the nonplanarity of the VO_4 fragment is responsible for d_{xy} and d_{z^2} orbital mixing, influencing the V═O−V interaction. Second, the P_2O_7 bridges explicitly included in our molecular models may account for an additional exchange interaction pathway. Experimental fits to inelastic neutron scattering[21] and light scattering[50] data suggested the presence of non-negligible ferromagnetic interactions ranging from −20 to −4 K. The interchain interactions modeled by D_{OPO}^C along the **b** direction

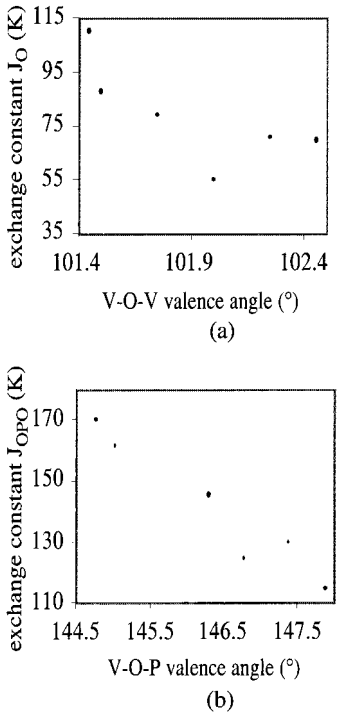

Figure 6. Exchange constant variations: (a) in D_O dimer as a function of V−O−V angle; (b) in D_{OPO} dimer as a function of V−O−P angle.

are approximately four times smaller than the ones along the **a** direction. As it has been shown in ref 42, the antiferromagnetic contribution to the total interchain exchange parameters is practically zero along the **a** direction and nonzero (though small) in the *bc* plane. As a result, the compensating effect on the dominating ferromagnetic component is weaker along the **a** direction.

As a main conclusion, our calculations confirm the very large anistropy of magnetic interactions in the $(VO)_2P_2O_7$ compound. Although the dimer chain model accounts for the most important interactions, there is no quantitative justification for completely neglecting the interchain magnetic couplings. Therefore, the model proposed in refs 50 and 51 for the APM phase of $(VO)_2P_2O_7$ seems to be the most adequate.

As far as intrachain interactions are concerned, O−P−O bridges provide much more efficient pathways than do μ-oxo bridges. As noticed in our previous study of the APM phase,[41] there is no direct correlation between the amplitude of exchange constants and the vanadium V−V distances. Indeed, the V−V distances in D_{OPO} vary in the range 5.13−5.18 Å as compared to 3.18−3.25 Å in D_O.

The model clusters **I** and **II** we used for D_{OPO} dimers exhibit qualitatively similar results for the absolute exchange values ordering. However, better agreement is reached with experimental exchange constants when one uses cluster **II**. This result demonstrates the crucial importance of the modelization of bridging units' coordination spheres. In that sense, all the nonbridging oxygen atoms of the PO_4 units must be saturated.

It is instructive to identify the structural parameters which may control the amplitude of coupling constants. The participation of several parameters (bond distances and valence angles) was investigated. If one is interested in obtaining a general trend, the most relevant are the V−O−V angle in D_O (Figure 6a) and

(50) Uhrig, G. S.; Normand, B. *Phys. Rev. B* **2001**, *63*, 134418.

(51) Uhrig, G. S.; Normand, B. *Phys. Rev. B* **1998**, *58*, R14705.

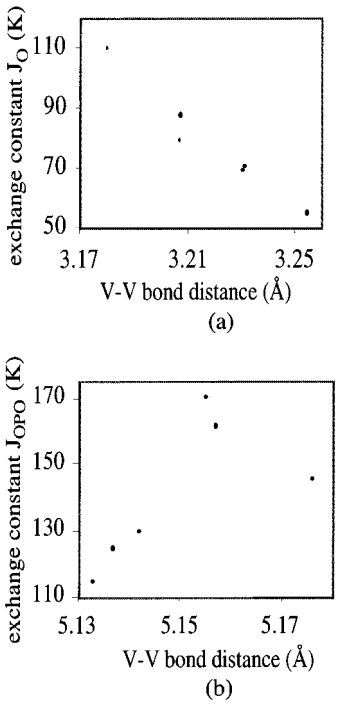

Figure 7. Exchange constant variations as a function of V−V distance: (a) in D_O and (b) D_{OPO} dimers.

the V−O−P angle in D_{OPO} (Figure 6b), where a quasi-linear dependency of exchange parameters is observed. The physical origin of such influence lies in the through-bond coupling between the two interacting vanadium centers. The angles involving the bridging units control the overlap efficiency between the vanadium and bridging oxygen orbitals.

However, the HPO phase constants slightly deviate from the general linear behavior. We may assume that the alternation up-down-up-down of vanadyl groups along the chain is responsible for this particular deviation.

The dependence of exchange parameters on V−V distances is quasi-linear in D_O dimers (Figure 7a). Conversely, for D_{OPO} dimers the amplitude of exchange constants does not monotonically decay with increasing vanadium V−V distance, a nonintuitive behavior (Figure 7b). As a matter of fact, in both APM and APO phases, the larger the V−V distance in D_{OPO} dimers, the greater the antiferromagnetic components. As this particular distance increases, one observes the displacements of the oxygen atoms toward the *x* and *y* axes, leading to a valence angle O−V−O close to 90°. The resulting enhanced overlap between metal d_{xy} and p_x (or p_y) oxygen is responsible for strong superexchange interaction, that is, antiferromagnetic coupling.

Concerning the methodological conclusions of our study, we must recall that the exchange parameters were calculated by means of eq 2, where the overlap integral was explicitly taken into account. These integrals between the magnetic orbitals are rather small ($S_{ab}^2 \ll 1$), and eq 4 corresponding to the localized limit seems to be a satisfactory approximation. It is now well-admitted that hybrid functionals are the most reliable theoretical approaches to calculation of exchange constants. Even though agreement between the experimental and the hybrid functional B3-LYP calculated values was reached for the μ_2-azido-bridged copper complex,[37] the same approach overestimated the exchange values by a factor of 2 for the μ_2-oxo copper complex.[47] The apparently good agreement between the experimental and B3-LYP results found for the μ_2-oxo copper complex in ref 35 is likely to arise from an error cancellation associated with an unjustified use of the delocalized picture (eq 3). Our results show that the reliability of a given theoretical approach strongly depends on the chemical nature of the system. For our particular vanadyl μ-oxo- and O−P−O-bridged systems, a combined B3-LYP/broken symmetry approach was found suitable to address the problem of calculation of exchange constants.

5. Conclusions

In this paper, the important issue of vanadyl pyrophosphate phase characterization was addressed by calculating exchange parameters. Although the three reported phases result from the same building units, small structural variations imposed by crystal lattice constraints can lead to significant changes in the strength of exchange couplings. Our calculations showed that the assumption of $(VO)_2P_2O_7$ being a strictly one-dimensional system is not completely justified. Vanadyl pyrophosphate phases are very different from one to another on the magneto-structural point of view. Magnetic properties could be used to trace the presence of different phases in a given system. In general, studies of catalytic systems based on vanadium phosphorus oxide phases would benefit a lot from the applications of magnetochemical methods. From the theoretical point of view, the estimation of exchange constants should lead to an improved analysis of NMR spectra.

Even though our calculations of exchange parameters were performed on the building units of a quite complicated solid, they reproduce the experimental values at a satisfactory level of accuracy. Therefore, molecular models can be reliable for the analysis of exchange interactions in three-dimensional solids. However, the choice of the model clusters as well as the use of a particular functional should be done with great care and might be limited to a given family of compounds.

JA011812D